Journal of Mines, Metals and Fuels, *73(3): 783-798; 2025. DOI: 10.18311/jmmf/2025/47760*

Print ISSN : 0022-2755

Journal of Mines, Metals and Fuels

**Contents available at:** *www.informaticsjournals.co.in/index.php/jmmf*

# Deep Learning-Based Detection and Classification of Moss and Crack Damage in Rock Structures for Geo-Mechanical Preservation

**P. Ramani[1], V. Reji[1], V. Sathish Kumar[2], G. Murali[3]* and Anant Sidhappa Kurhade[4]**

*[1]Department of Electronics and Communication Engineering, SRM Institute of Science and Technology, Ramapuram, Chennai - 600089, Tamil Nadu, India*

*[2]Department of Electronics Engineering, MIT Campus, Anna University, Chromepet - 600044, Chennai, India*

*[3]Department of Mechanical Engineering, Koneru Lakshmaiah Education Foundation, Green Fields, Vaddeswaram, Guntur (Dt) - 522502, Andhra Pradesh, India*

*[4]Department of Mechanical Engineering, Dr. D. Y. Patil Institute of Technology, Sant Tukaram Nagar, Pimpri, Pune - 411018, Maharashtra, India; a.kurhade@gmail.com*

## Abstract

*Stone monuments, valuable cultural assets that inspire thoughts of expression and legacy, necessitate effective preservation strategies. This research proposes a novel approach utilizing Deep Learning for automated detection, classification, and evaluation of moss and crack damage. The methodology involves fusing Luminance with Gray-Level Co-occurrence Matrices (GLCM) for data analysis. Monument decay is then classified using a Multi-Layer Neural Network (MLNN) and rigorously validated using metrics such as precision, selectivity, sensitivity, and accuracy. Damage assessment employs indices and categories, with spread parameters evaluating crack damage and colour change levels assessing moss damage. The estimated damage severity guides the design of appropriate recovery and preservation plans. Notably, this innovative method achieves a high classification accuracy of 97% for monument decay, demonstrating its potential for significantly improving the long-term preservation of these invaluable cultural treasures.*

***Major Findings:*** *This research presents a novel deep learning-based model for automated detection and classification of moss and crack damage in stone monuments, achieving a high classification accuracy of 97%. The model effectively assesses decay parameters using an MLNN, demonstrating superior performance compared to existing methods like Local Binary Patterns, with high G-mean, Precision, Specificity, Accuracy, F-measure, and Sensitivity values. The model provides valuable insights for monument preservation by generating damage maps, identifying damage categories and indices, and estimating damage severity, guiding the development of effective recovery and preservation plans.*

**Keywords:** *Decay Assessment, Decay Categorization, Deep Learning, GLCM, MLNN*

## 1.0 Introduction

India as a nation has an extensive and noteworthy history as well as a magnificent legacy. Its distinctive culture and customs are widely observed worldwide. There are unique heritage architecture, customs, and cultural practices in every region of this nation. Sadly, after being subjected to environmental changes for thousands of years, cultural heritage sites suffer significant harm. Before organizing the restoration work, a weathering deterioration

**Author for correspondence*

evaluation is required for the conservation of historic buildings. Destruction of stone structures can appear in different forms, with various types of damages caused by its environments such as storms, fire, temperature, rain, floods, and biological colonization, such as fungi, alga, lichen, and moss[1].

Physical, biological, chemical, structural and artificial are different weathering forms. Physical weathering, due to four seasons during the year, causes damage to the object exposure on the site. Peeling, exfoliation, and degradation occur in monuments due to the rain and the wind action of natural weather[2-6]. Deformation or cracks in the stone position are shifted due to structural factors. Displacement is one example of this weather[7]. Chemical weathering is caused due to various components (like S, $CO_2$, $SO_4$, $SO_2$, and NO) dissolved in rainwater, surface, or groundwater that decompose the configuration of rock chemicals. Chemicals that react with water on the stone surface produce rock yellow, brown, white, and discolouration of the stone[8-10].

Artificial factors cause some rock damage due to artificial colouring and paint colouring. Decay is a natural process that occurs on monuments due to weathering. There are two types of decay analysis such as destructive and non-destructive types. In the destructive type, the samples were removed from the site for laboratory analysis. The Non-destructive type is the process of testing or inspecting the components without destroying the characteristics or part of the system.

Drilling resistance measurement, scanning electron microscopy, water uptake, and X-ray diffraction are destructive methods[11-13]. The traditional approach to assessing degradation entails gathering samples from the location and performing laboratory analyses. Those invasive techniques are unsuitable and inappropriate for precious, treasured historical monuments. The non-destructive methods are Eddy current, penetrant, radiographic, ultrasonic testing, infrared thermography, and digital image processing and deep learning methods[14-23].

Non-destructive techniques automatically process the image to extract valuable data. It extracts, categorizes, and recognizes surface patterns on digital images by applying image processing operations using software[24–27]. It provides a detailed mapping of conservation and intervention compatibility. Destructive testing requires a lot of time and resources. Digital image processing and deep learning is one type of non-destructive method, and it is a simpler and less time-consuming method[28] than other existing methods.

In this research, a fused luminance with grey level concurrence matrix pattern method has been proposed to detect the type of decay and a novel decay assessment method has been developed to detect the severity of the decay. This paper is organized as follows: section 2 describes the aim of the research, section 3 summarizes the pertinent work, section 4 presents the proposed work, section 5 explains the results and discussions, and section 6 outlines the conclusion and future work.

### 1.1 Significance of the Case Study

Stone monuments are invaluable treasures within the world's cultural heritage. Many centuries old, these artefacts face significant environmental degradation. They hold invaluable information about our country's rich history, including contributions to music, astronomy, medicine, and dance. Destructive methods for assessing decay in these ancient monuments are not viable.

This research proposes a technological solution using non-destructive methods to assess the decay of these monuments. Despite the advanced architectural and construction practices of ancient India, environmental changes over the centuries have severely impacted these heritage structures. While numerous heritage structures exist across the country, many lack proper maintenance, particularly those associated with religious centers that often lack a scientific approach to conservation.

Scientific interventions are crucial for assessing weather patterns and the extent of damage to these structures. These interventions must be non-destructive, conducted on-site, efficient, and cost-effective, ideally providing graphical maps of damaged locations and distributions. This information is essential for developing effective restoration and preservation plans.

## 2.0 Research Aim

No prior studies have used the deep learning method to assess monument decay. This research aims to develop

a non-destructive deep learning algorithm that can automatically detect and assess both moss and crack decay of cultural heritage structures.

This research aims to acquire high-resolution digital images of decaying monument surfaces using a high-resolution camera. Subsequently, it will develop and implement deep learning algorithms to analyze the extracted features from these images, enabling the identification and assessment of various weathering forms and the extent of weathering damage on the ancient structures. The analysis will also facilitate the mapping of decayed areas on the monument surfaces.

## 3.0 Literature Survey

Historical cultural heritage structures are decayed by the environment, man, rain, and other parameters. In the proposed work, the decay process and the crack that develops in structures like beams concretes have been discussed. The development of cracks is a result of constant stress on structures like beams and concrete structures, which decay because of cyclic loading. Consequently, early detection of these failures is critical to preserving historic monuments and their locations, and this section has covered a thorough review of destructive and non-destructive techniques. In 2018, Brooks created a model for identifying cracks equipped with thermal cameras. The camera was utilized to detect the deformities in large outside regions as well as to differentiate the impression of an infrared source from the crack's exterior. Using the Make3D toolkit, proposed a novel approach for estimating crack depth[29].

2D photos had been transformed into 3D images using the toolbox. Using supervised learning, the model was trained and classified using ground truth values obtained from the laser scanner[30]. Aslam *et al.,* developed a new technique for assessing metal imperfections in terms of size, measurements, and shape. The noises were removed by median filtering. Segmentation and recognition of the damage of metal using CNN had achieved a 93% accuracy rate[31] attained with the proposed effort. The multi-class support vector machine classifies decay and validates and evaluates the performance based on sensitivity, precision, accuracy, etc. The proposed method of this research gives better results than the existing method[32]. To remove human error from historical stone monuments, Hatir *et al.,* have created an AI-based recognition technique. They classified the different weathering decays using deep learning techniques and achieved 99%, but most decay analysis was not done[33]. Jaiswal *et al.,* implemented monument detection using the VGG-16 and Yolo V5 algorithms. This method proposed by Yolo gives 90% accuracy, while using VGG-16 gives 63% accuracy for 200 iterations[34]. Bruno *et al.*, presented a novel approach that makes use of the mask R-CNN method to identify decay morphologies. The experiment was carried out using a heterogeneous dataset. This method provides an average precision of 77% for biological colonization decay[35]. Ramani *et al.*, used an LBP with the luminance method, and thus the efficiency of crack and moss detection had improved. With the suggested approach, a 97% accuracy rate was attained[36]. Ramani *et al.*, discussed various classification methods to detect decay, such as cracks, moss, or loss of stone.

The different deep learning techniques are explained to detect the type of decay using invasive and non-invasive methods[37]. Diagnosis is the crucial step for the improvement of logical information concerning deterioration. Regarding monument safeguarding, analysis is important for the well – well-acknowledged way to deal with monument protection. Damage finding is required for complete portrayal, rating and interpretation of the cultural structures. *In situ,* examination of monuments makes a significant commitment to damage analysis on stone. Analysis is crucial for the improvement of logical information concerning stone decay. The ensuing utilization of weathering forms, damage classifications, and indices lists permit complex logical and common sense assessment[38]. These structures are used for point-by-point objective and reproducible depiction of individual decay phenomena at the mesoscale according to the intensity and type. The proposed method performs both assessment and detection of decay.

## 4.0 Materials and Methods

High-resolution images were captured using a Canon Eos 7D Digital SLR camera from various cultural heritage sites in Tamil Nadu, including Sivapuram, Kooram Temple, and Mahabalipuram Temple. This section is divided into two parts: the first part outlines the methods used to detect moss and cracks in the captured images,

while the second part explains the system for classifying and categorizing the detected damage, including the development of damage indices.

## 4.1 Proposed Crack/Moss Detection

5184 x 3456 is the pixel size of the acquired image. After being scaled to 256 by 256, the acquired images are preprocessed. The RGB colour image is then transformed into a grayscale and YCbCr image. Picture Y represents the image's luminance, which provides information on brightness in terms of grayscale black and white hues. Figure 1 shows the proposed decay detection approach.

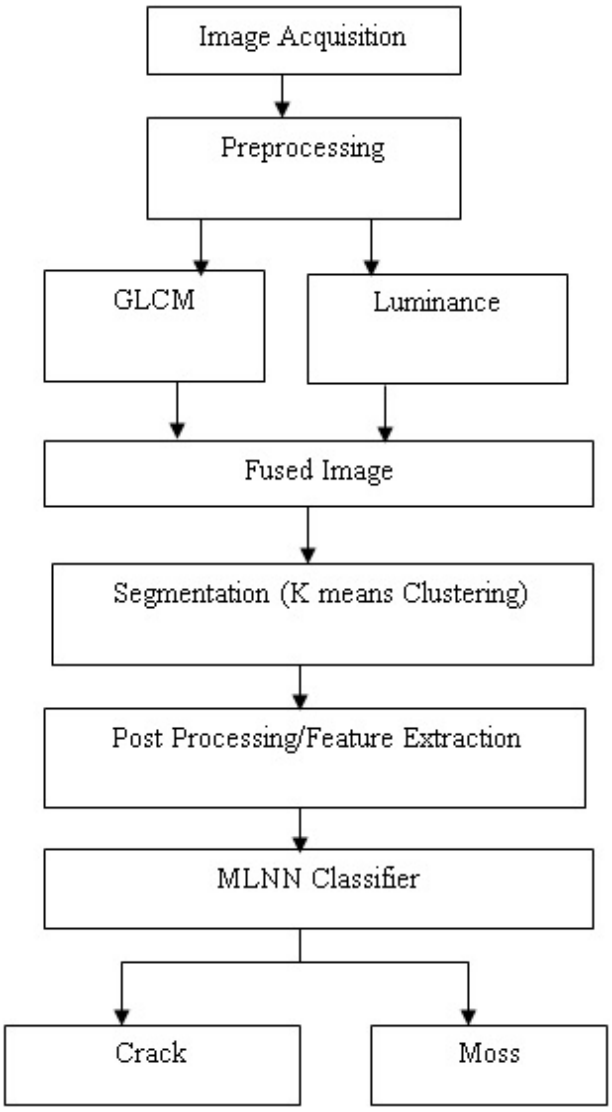



**Figure 2.** The proposed method of decay detection.

The grey images are applied as input to GLCM. GLCM is among the techniques for extracting textures. The concept of the GLCM method is given as follows:

It computes the statistical distribution of intensities infusion at a particular position in the image. The order for the measurements is settled relies upon the quantity of contributing intensity in the combination. The second-order surface features are extricated by taking the spatial relationship of continuous intensity values. It is the main strategy to bring out surface data[39]. As a component of its grey level, GLCM illustrates how each grey level regularly occurs at a pixel coordinated at a constant mathematical position relative to one another pixel[40]. It is among the techniques for extracting textures. These extracted texture features are called Haralick features. Following the combination of GLCM and luminance images, K-means clustering was performed to segment the fused images.

### *4.1.1 K-means Clustering*

It's that kind of unsupervised method. It segments the image by classifying each pixel in the class with the nearest mean, then grouping the data by repeatedly calculating an average intensity for each class[41].

The processes needed to carry out the clustering are

(a) Determine the number of clusters at random first.
(b) Group the pixels into a K-cluster.
(c) Next, compute the cluster's mean value.
(d) Assign the objects closer to the cluster after determining which pixels are closest to them.
(e) Steps c and d should be repeated until the centroid remains unchanged.

This study investigates five distinct weathering forms. Following image segmentation, noise reduction is applied through post-processing. Statistical properties, including kurtosis, mean, skewness, variance, and entropy, are extracted from the segmented image's histogram. To assess and detect moss or fractures, Mean Squared Error (MSE) and Peak Signal-to-Noise Ratio (PSNR) metrics are employed. These metrics are also calculated for both fused Local Binary Patterns (LBP) with luminance and Gray-Level Co-occurrence Matrices (GLCM) with luminance. Representative images and their corresponding MSE and PSNR values are tabulated. Image quality is quantified using Equations 1 and 2.

$$\text{MSError}=\frac{\left[\text{Im}(c,d)-\overline{\text{Im}(c,d)}\right]^2}{M} \quad (1)$$

$$\text{PSNR}=10\log_{10}\left(\frac{S^2}{MSError}\right) \quad (2)$$

I'm(c,d)=test pixels

$\overline{\text{Im}(c,d)}$ = noisy pixels

S- Total pixels on an image
M, N – Row and Column of the image

Table 1 compares the PSNR of the fused image with LBP-Luminance and GLCM-Luminance. The quality parameter of the proposed method gives better accuracy than the existing method.

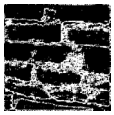
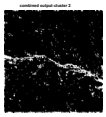
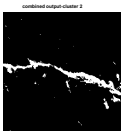
### *4.1.2 Multi-Layer Neural Network*

The MLNN classifier utilizes statistical features as input to categorize test images as either cracks or moss. To enhance classification accuracy, the model is trained with ten hidden layers.

## 4.2 Damage Assessment

In the second part, 100 images are taken as training images and **35** as test images. The images are classified as cracks or moss using deep learning techniques. Figure 2

**Table 1.** Comparison of the quality parameter of the proposed method of LBP

| Original Image | Fused Image (LBP+Luminance) | | Fused Image (GLCM+Luminance) | |
|---|---|---|---|---|
| | Image | PSNR | Image | PSNR |
| **Moss**  |  | **8.88** |  | **13.69** |
| Moss  |  | **8.21** |  | **13.4** |
| **Crack**  |  | **9.3** |  | **13.92** |
| **Crack**  |  | **9.25** |  | **13.97** |

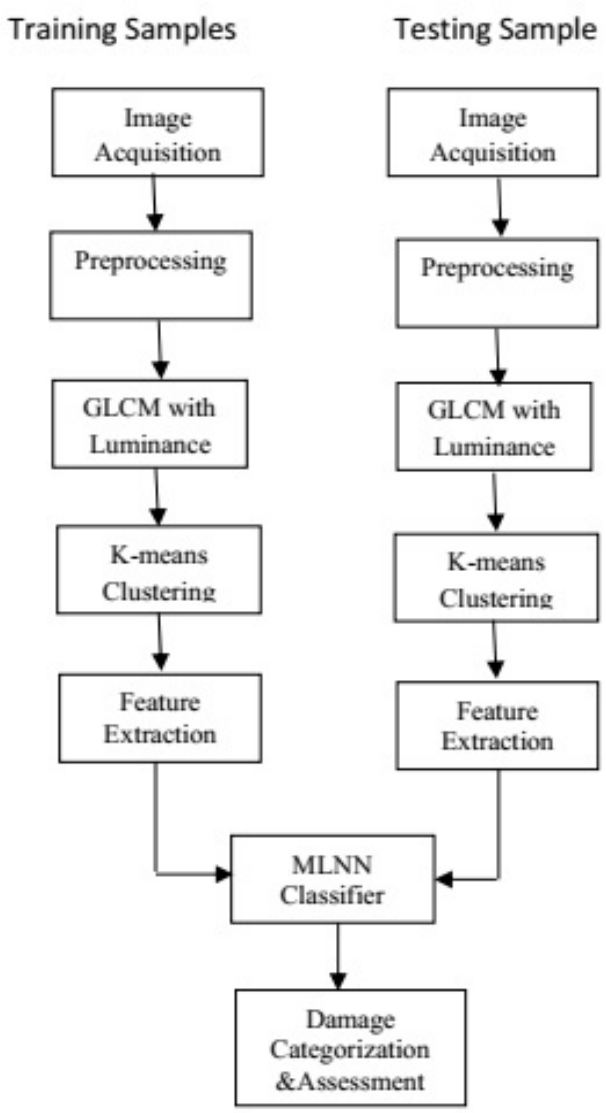



**Figure 2.** Proposed approach to decay assessment.

presents the proposed approach to decay categorization and assessment.

Following the classification, the images are categorized, and the decay is evaluated. MATLAB coding has been developed for damage categorization, quantification, and rating. Stone damage evaluation is done based on weathering forms according to type, colour, and intensity[42]. Several weathering factors, including rain, wind, temperature changes, storms, flooding, and fire, can cause monuments to deteriorate[43]. Three types of weathering are responsible for deterioration: chemical, biological, and physical. The elements of a cultural heritage structure that are deteriorating are the moss and cracks. Weathering forms provide an accurate representation of stone deterioration. Damage categorization has been devised to assign a numerical value to each damage. The provided formula is used to compute the affected or degraded area.

$$\text{Degraded Area} = \frac{Affected\ Area}{Total\ Area} \quad (3)$$

There are four different categories of damage. Categorization 0 indicates no visible damage, 1 indicates slight damage, 2 indicates moderate damage, and 3 indicates severe damage.

For most images, damages are classified according to the extent of colour changes, and for crack images, the spread parameters of the crack are used for classification. Damage indices are a definitive way to rate and quantify stone damages. The monument must be immediately cleaned to save the treasure if it comes under category 3. Chemical cleaning and Water pouring are the two different methods to preserve the monuments. Damage categorizations have been characterized to rate the damage and discussed in the following section.

### *4.2.1 Moss Categorization*

The monuments are categorized once the classification is done. Moss in the monument is categorized by the level or degree of colour changes. Naturally, the colour of moss lies from light green to dark green. The RGB intensity range is used to define the degree of colour variation. Min and Max RGB colour is used to categorize the most damage. The severity of moss is characterized by pixel values of these three colours. The dark green colours denote severe damage, and light green is categorized as light damage.

The minimum and maximum RGB range of moss in monuments was calculated and moss decay is categorized into four types based on the three-color ranges. The RGB value between [91 93 100] and [250 250 250] indicates no visible damage, while values between [90 120 40] and [160 195 95] indicate slight damage, values between [40 50 30] and [60 88 52] indicate moderate damage, and values between [10 10 10] and [67 78 96] denote moderate

**Table 2.** Damage categories of moss with RGB values

| Moss Image | Damage Category | RGB Values |
|---|---|---|
|  | Severe Damage | [41,31,19] |
|  | Slight damage | [102,125,83] |
|  | Moderate damage | [59,54,50] |
|  | Severe Damage | [37 35 31] |
|  | No visible damage | [198,145,106] |

damage. Table 2 shows the images of the damage category 0–3 with corresponding RGB values. Light green damage indicates moderate damage. Severe damage is indicated by its dark colour.

### *4.2.2 Crack Categorization*

Crack classification is performed using the spread parameter of moments, calculated from shape descriptors

that characterize specific geometric qualities of features. 2. Higher-order moments reveal fine details, while lower-order moments describe basic properties and are expressed in equation 6.2. 3. Moments are image features enabling geometric image reconstruction[44]. 4. The zero-order moment determines the object's area, while the first-order moment locates the centre of mass. 5. The second order describes the difference

**Table 3.** Damage categories of crack with spread values

| Moss Image | Damage Category | Spread |
|---|---|---|
|  | Severe type | 0.623 |
|  | Slight type | 7.935 |
|  | Moderate type | 2.4 |
|  | Severe type | 0.318 |
|  | No Visible type | 15 |

between the centroids. 6. The third-order moment defines skewness, indicating the proportion of deviations from mean evenness. 7. The fourth-order moment defines kurtosis, indicating the peakiness or flatness of the distribution. 8. Any image can be fitted into an ellipse, and its regional properties, such as minor and major axis lengths and area, can be determined from moments[45, 46].

A moment with an order of (p,q) is as follows.

$$m_{pq} = \sum_{xi=0}^{N-1} \sum_{yi=0}^{M-1} xi^{p}\, yi^{q} f(xi, yi) \tag{4}$$

Zeroth order moment

$$m_{00} = \sum_{xi=0}^{N-1} \sum_{yi=0}^{M-1} xi^{0}\, yi^{0} f(xi, yi) \tag{5}$$

Where M=N

Centroid is calculated from the first-order moment[47]

$$xi_0 = \frac{m_{10}}{m_{00}} \qquad \mathrm{yi}_0 = \frac{m_{01}}{m_{00}} \tag{6}$$

Moment of Inertia along X and Y direction

$$I_1 = \frac{(\mu_{20} + \mu_{02}) + \left[(\mu_{20} - \mu_{02})^2 + 4\mu_{11}^2\right]^{1/2}}{2} \tag{7}$$

$$I_2 = \frac{(\mu_{20} + \mu_{02}) + \left[(\mu_{20} - \mu_{02})^2 + 4\mu_{11}^2\right]^{1/2}}{2} \tag{8}$$

Orientation

$$\theta = \frac{1}{2}\tan^{-1}\left(\frac{2\mu_{11}}{\mu_{20} - \mu_{02}}\right) \tag{9}$$

$$a = 2\left(\frac{I_1}{\mu_0}\right)^{1/2}, \quad \mathrm{b} = 2\left(\frac{I_2}{\mu_0}\right)^{1/2} \tag{10}$$

$$spread = \left(\frac{I_1 + I_2}{m_0^2}\right) \qquad elongation = \left(\frac{I_2 - I_1}{I_1 + I_2}\right) \tag{11}$$

Moments were calculated using a and b values. Spread is determined by moments and crack categorization is implemented using the spread parameter. The spread value categorizes crack damage.

A spread value greater than 10 indicates damage Category 0.

The spread value from 5 to 9 indicates damage category 1.

A spread value ranging from 1 to 5 indicates damage Category 2.

The spread value from 0 to 1 indicates damage category 3.

The categorization of crack is done using the spread parameter. Table 3 shows the images under categories 0-3 with corresponding spread values.

### 4.2.3 Damage Indices

The utilization of damage indices provides a rating and examination of materials concerning their vulnerability to degradation. Damage indices call attention to the need and earnestness of mediation. Damage categorization finds those pieces of the monument that need to be focused on. Weathering forms must be considered for the allowance of proper kinds of protection measures. Indices and categorization of damage speak to exceptionally reasonable apparatus for solid judgment/confirmation of conservation measures.

Damage indices characterized the decisive evaluation and rating of weathering damage at monuments[48]. The figuring of this list depends on the quantitative assessment of damage categorization.

Damage indices are determined from categories of damage. It is divided into two categories. There are two types of damage indices: the Progressive damage index and the linear damage index. The average decay category is called LDind. The percentage of higher damage categories is shown by the progressive damage index. Equations 12 and 13 are utilized to calculate these indices. The interval spans from 0 to 3.

$$\mathrm{LD}_{\mathrm{ind}} = \frac{(Ai.0) + (Bi.1) + (Ci.2) + (Di.3)}{100} \tag{12}$$

$$\mathrm{PD}_{\mathrm{ind}} = \frac{\sqrt{(Ai.0) + (Bi.1) + (Ci.4) + (Di.9)}}{100} \tag{13}$$

Where

$$Ai = Area(\%)\ of\ \ NoVisible\ Damage$$
$$Bi = Area(\%)\ of\ \ Slight\ \ Damage$$
$$Ci = Area(\%)\ of\ \ Moderate\ Damage$$
$$Di = Area(\%)\ of\ \ Severe\ Damage$$

$$\sum_{Ai}^{Di} = 100$$

For different stone monuments, damage indices will be determined exclusively to analyze and rate their susceptibility and, afterwards, generate a colour-coded image.

## 5.0 Results and Discussion

The work is done in MATLAB 2020b with Windows 10. A total of 100 training samples and 35 test samples were used for this analysis. Features are extracted after the segmentation process. The ageingous phases of the detected moss image using fused GLCM with luminescence are shown in Figure 3.

The decay parameters are detected, and the quality is analyzed with MSE and PSNR. These fused images are segmented using K-means clustering. Statistical features are extracted after the clustering process. Then the features of the moss and crack images are classified using MLNN.

Table 4 presents the performance metrics of the proposed approach in comparison to the current method. It can be observed that the new method yields superior outcomes.

**Table 4.** Performance metrics of the proposed method with fused LBP

| Parameters | Different Feature Extraction Methods | |
|---|---|---|
| | Luminance plus LBP | Luminance plus GLCM |
| Sensitivity | 95.7% | 98.50% |
| G mean | 94.99% | 97.84% |
| Precision | 94.3% | 97.2% |
| Accuracy | 93.0% | 97.0% |
| F measure | 94.99% | 97.99% |
| Specificity | 86.60% | 93.1% |

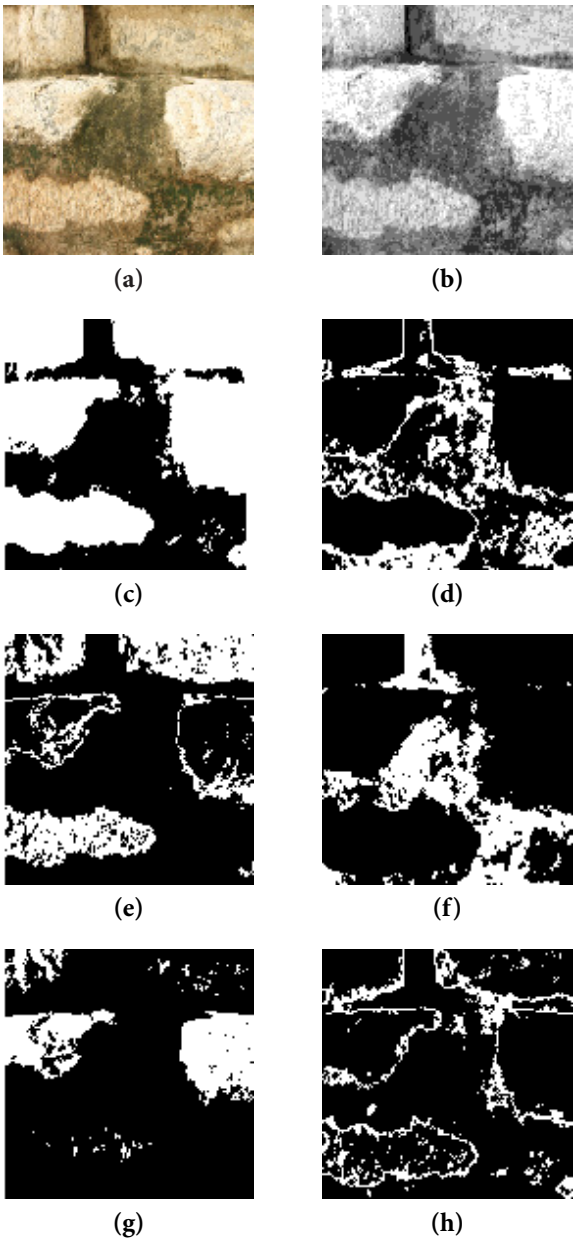



**Figure 3.** GLCM plus Luminance – **(a)** Test image, **(b)** Luminance of test image **(c)** Fused image **(d)** to **(f)** Cluster 1 to 5.

**Table 5.** Comparison between different existing crack detection methods with the proposed method

| Existing | Techniques used | Accuracy |
|---|---|---|
| Pingrang Wang *et al.,* (2010) | Integrated Thresholding segmentation[49] | 91% |
| Zhang Wenyu *et al.,* (2014) | Morphological image processing techniques and Thresholding[50] | 90% |
| Ikhlas Abdel-Qader *et al.,* (2016) | Fast Haar Trasform[51] | 86% |
| Zhang, Yi Xiang, *et al.,* (2016) | LBP and BPNN[52] | 93% |
| Aradhya Saini *et al.,* (2017) | Deep Convolutional Neural Networks (DCCN)[53] | 92.7% |
| Krisada Chaiyasarn *et al.,* (2018) | CNN and SVM[54] | 85.9% |
| Manjurul Islam (2019) | DCCN using FCN (Fully Convolutional Neural) Networks[55] | 92% |
| Aslam Y *et al.,* (2020) | Supervised approach with CNN[56] | 93% |
| Feng, Chuncheng, *et al.,* (2020) | Deep Convolutional Network[57] | 90% |
| Proposed Method | Deep Learning Approach with Integrated GLCM - Luminance | 97% |

**Table 6.** Damage indices and category

| Input Image | Proposed -Crack image | Spread | Elongation | Orientation | Damage Category | Damage Area | Damage Indices |
|---|---|---|---|---|---|---|---|
|  |  | 2..847 | 0.99 | - 83.37 | 2-Moderate Damage | 2269 | $L_{ind}$ =0.07$P_{ind=}$ 0.39 |
|  |  | 7.935 | 0.98 | -85.377 | 1-Slight Damage | 779 | $L_{ind}$ =0.013$P_{ind}$ =0.03 |

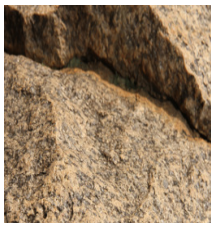
| | | | | | | | |
|---|---|---|---|---|---|---|---|
|  |  | 2.73 | 0.99 | 86.46 | 2-Moderate damage | 1821 | $L_{ind}$ =0.06$P_{ind}$ =0.354 |
|  |  | 0.393 | 0.6 | 80.55 | 3-Severe Damage | 12175 | $L_{ind}$ =0.61$P_{ind}$ =1.36 |
|  |  | 0.318 | 0.78 | -21.02 | 3-Severe Damage | 15704 | $L_{ind}$ =0.79$P_{ind}$ =1.6 |
|  |  | 2.4 | 0.8 | 5.3 | 2-Moderate Damage | 2185 | $L_{ind}$ =0.11$P_{ind}$ =0.57 |

Table 5 describes the comparison of different crack detection methods with the proposed method using image processing techniques and deep learning techniques. The various image segmentation algorithms for the detection of cracks, such as integrated thresholding, morphological techniques, fast haar transform, CNN, and a supervised approach with CNN,–are used in all existing methods, whose classification accuracy rate was less than 97% compared to the proposed method.

Table 6 shows the Linear and progressive damage indices of cracks. The fourth and fifth images in the table below have a higher damage index and come under severe damage. This needs to be immediately restored to save the cultural heritage structures.

The colour-coded images of two decays are shown in Figure 4. The minimum damage is described by the lower damage index, and it requires carrying out preservation methods. Severe damage denotes the higher damage category, and it is necessary to perform the restoration. The use of damage indices permits invariable measurement and rating of damages that contribute to heritage structure protection.

## 6.0 Conclusion

Stone monuments are susceptible to various forms of weathering. While manual damage detection is time-

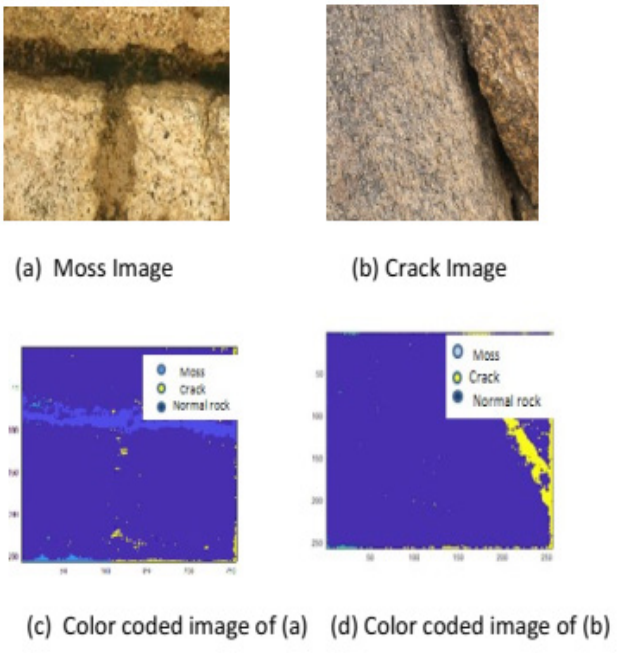



**Figure 4.** Moss and crack of a colour-coded map.

consuming, this research proposes an automated approach using image processing and deep learning. The developed model effectively detects different types of decay, such as cracks and moss, demonstrating superior performance compared to existing methods like Luminance with GLCM and LBP.

The model achieves high accuracy in decay parameter assessment using an MLNN, with G-mean, Precision, Specificity, Accuracy, F-measure, and Sensitivity values exceeding those of the Local Binary Pattern. Damage is categorized and indexed, with most damage assessed based on modelling and crack damage assessed based on spread values.

The estimated damage severity highlights the need for immediate intervention. Damage maps pinpoint specific areas requiring urgent attention. The type and extent of damage guide the selection of appropriate preservation techniques. This research focuses on a single non-destructive method. Future studies will incorporate other weathering forms and explore alternative detection methods, including IRT, Ultrasonic Imaging, LIDAR, and advanced image processing techniques, to comprehensively assess the depth of decay within the monuments.

## 7.0 Acknowledgement

We are appreciative that the Tamil Nadu Department of Archaeology allowed us to take pictures at various historic temples.

## 8.0 References

1. Mérillou S, Ghazanfarpour D. A survey of ageing and weathering phenomena in computer graphics. Computers and Graphics. 2008; 32(2):159-74. https://doi.org/10.1016/j.cag.2008.01.003
2. Fitzner B, Heinrichs K, Kownatzki R. Weathering forms at natural stone monuments-classification, mapping and evaluation. Int J Rest Build Mon. 1997; 3:105-24. https://doi.org/10.1515/rbm-1997-0204
3. Schaffer RJ. The weathering of natural building stones. Routledge; 2016. https://doi.org/10.4324/9781315793771
4. Fitzner B, Heinrichs K. Photo atlas of weathering forms on stone monuments. Geological Institute, RWTH Aachen University-Working Group Natural stones and weathering; 2004.
5. Ema NP, de Buergo MA, Bustamante R. Effects of conservation interventions on the archaeological Roman site of Merida (Spain). Advance of research. Procedia Chemistry. 2013; 8:269-78. https://doi.org/10.1016/j.proche.2013.03.033
6. Hatir ME, Barstuğan M, İnce İ. Deep learning-based weathering type recognition in historical stone monuments. Int J Cult Herit. 2020; 45:193-203. https://doi.org/10.1016/j.culher.2020.04.008
7. Price CA. Stone Conservation: An Overview of Current Research. Getty Conservation Institute; 2011.
8. Bandeira D, Walter M. Highlights on weathering effects: Improving the appearance modelling of weathering effects on images. The Visual Computer. 2010; 26:965-74. https://doi.org/10.1007/s00371-010-0495-1
9. Mérillou S, Ghazanfarpour D. A survey of ageing and weathering phenomena in computer graphics. Computers and Graphics. 2008; 32(2):159-74. https://doi.org/10.1016/j.cag.2008.01.003
10. Verstrynge E, Adriaens R, Elsen J, Van Balen K. Multi-scale analysis on the influence of moisture on the mechanical behaviour of ferruginous sandstone. Constr Build Mater. 2014; 54:78-90. https://doi.org/10.1016/j.conbuildmat.2013.12.024

11. Dong J, Kim B, Locquet A, McKeon P, Declercq N, Citrin DS. Nondestructive evaluation of forced delamination in glass fibre-reinforced composites by terahertz and ultrasonic waves. Compos B Eng. 2015; 79:667-75. https://doi.org/10.1016/j.compositesb.2015.05.028
12. Péronnet E, Eyma F, Welemane H, Mistou S. Characterization and comparison of defects detection limits of ultrasonic non destructive techniques. Key Eng Mater. 2012; 498:79-88. https://doi.org/10.4028/www.scientific.net/KEM.498.79
13. Fais S, Casula G, Cuccuru F, Ligas P, Bianchi MG. An innovative methodology for the non-destructive diagnosis of architectural elements of ancient historical buildings. Sci Rep. 2018; 8(1):4334. https://doi.org/10.1038/s41598-018-22601-5
14. Ghoshal A, Ayers J, Gurvich M, Urban M, Bordick N. Experimental investigations in embedded sensing of composite components in aerospace vehicles. Compos B Eng. 2015; 71:52-62. https://doi.org/10.1016/j.compositesb.2014.10.050
15. Montoto M, Calleja L, Perez B, Esbert RM. Evaluation in situ of the state of deterioration of monumental stones by non-destructive ultrasonic techniques. MRS Online Proceedings Library (OPL). 1990; 185:273. https://doi.org/10.1557/PROC-185-273
16. Nappi A, Cote P. Nondestructive test methods applicable to historic stone structures. Environmental Sciences Research Report ES. 1997; 20:151-66.
17. Tian XL, Zhou X, Gao F. Nondestructive testing and analysis technology in the field of heritage preservation. Nondestructive Testing. 2008; 30(3):178-82.
18. Mishra M, Bhatia AS, Maity D. Support vector machine for determining the compressive strength of brick-mortar masonry using NDT data fusion (case study: Kharagpur, India). SN Appl Sci. 2019; 1(6):564. https://doi.org/10.1007/s42452-019-0590-5
19. Mishra M, Bhatia AS, Maity D. A comparative study of regression, neural network and neuro-fuzzy inference system for determining the compressive strength of brick-mortar masonry by fusing nondestructive testing data. Engineering with Computers. 2021; 37(1):77-91. https://doi.org/10.1007/s00366-019-00810-4
20. Pascale G, Lolli A. Crack assessment in marble sculptures using ultrasonic measurements: Laboratory tests and application on the statue of David by Michelangelo. Journal of Cultural Heritage. 2015; 16(6):813-21. https://doi.org/10.1016/j.culher.2015.02.005
21. Martinho E, Dionísio A, Almeida F, Mendes M, Grangeia C. Integrated geophysical approach for stone decay diagnosis in cultural heritage. Construction and Building Materials. 2014; 52:345-52. https://doi.org/10.1016/j.conbuildmat.2013.11.047
22. Tavukçuoğlu A. Mapping of visual decay forms and infrared imaging of stone structures for the maintenance and monitoring studies.
23. Salman M, Mathavan S, Kamal K, Rahman M. Pavement crack detection using the Gabor filter. In: 16th International IEEE Conference on Intelligent Transportation Systems (ITSC 2013). 2013; 2039-2044. IEEE. https://doi.org/10.1109/ITSC.2013.6728529
24. Jain AK. Fundamentals of digital image processing. Prentice-Hall, Inc.; 1989.
25. Schalkoff RJ. Digital image processing and computer vision. New York: Wiley; 1989.
26. Jung H, Lee C, Park G. Fast and non-invasive surface crack detection of press panels using image processing. Procedia Eng. 2017; 188:72-9. https://doi.org/10.1016/j.proeng.2017.04.459
27. Pragalath H, Seshathiri S, Rathod H, Esakki B, Gupta R. Deterioration assessment of infrastructure using J Perform Constr Facil. 018009. https://doi.org/10.1061/(ASCE)CF.1943-5509.0001151
28. Moropoulou A, Koui M, Theoulakis P, Kourteli C, Zezza F. Digital image processing for the environmental impact assessment on architectural surfaces. J Environ Chem. 1995; 2:343-50.
29. Brooks AJ, Hussey DS, Yao H, Haghshenas A, Yuan J, LaManna JM, Jacobson DL, Lowery CG, Kardjilov N, Guo S, Khonsari MM. Neutron interferometry detection of early crack formation caused by bending fatigue in additively manufactured SS316 dogbones. Mater Des. 2018; 140:420-30. https://doi.org/10.1016/j.matdes.2017.12.001
30. Shehata HM, Mohamed YS, Abdellatif M, Awad TH. Depth estimation of steel cracks using laser and image processing techniques. Alex Eng J. 2018; 57(4):2713-8. https://doi.org/10.1016/j.aej.2017.10.006
31. Aslam Y, Santhi N, Ramasamy N, Ramar K. Localization and segmentation of metal cracks using deep learning. J Ambient Intell Humaniz Comput. 2021; 12:4205-13. https://doi.org/10.1007/s12652-020-01803-8
32. Benco M, Hudec R, Kamencay P, Zachariasova M, Matuska S. An advanced approach to the extraction of colour texture features based on GLCM. International

Journal of Advanced Robotic Systems. 2014; 11(7):104. https://doi.org/10.5772/58692
33. Hatir ME, Barstuğan M, İnce İ. Deep learning-based weathering type recognition in historical stone monuments. J Cult Herit. 2020; 45:193-203. https://doi.org/10.1016/j.culher.2020.04.008
34. Jaiswal GK, Student HM, Chaudhary R, Kumar M. Identification of monuments from aerial images using deep learning techniques. International Journal of Engineering Applied Sciences and Technology. 2023; 8(2):123-129.
35. Bruno S, Galantucci RA, Musicco A. Decay detection in historic buildings through image-based deep learning. VITRUVIO-International Journal of Architectural Technology and Sustainability. 2023; 8:6-17. https://doi.org/10.4995/vitruvio-ijats.2023.18662
36. Perumal R, Venkatachalam SB. Non-invasive decay analysis of monument using deep learning techniques. Traitement du Signal. 2023; 40(2):639-46. https://doi.org/10.18280/ts.400222
37. Ramani P, Subbiah Bharathi V, Sugumaran S. Non-destructive analysis of crack using image processing, ultrasonic and IRT: A critical review and analysis. In: International Conference on Cognitive Computing and Cyber-Physical Systems. 2022; 144-155. Cham: Springer Nature Switzerland. https://doi.org/10.1007/978-3-031-28975-0_12
38. Kilian J. Simple image analysis by moments [Internet]. Open CV library documentation; 2001.
39. Devesh R, Jha J. An efficient approach for monuments image retrieval using multi-visual descriptors. In: Proceedings of the Second International Conference on Microelectronics, Computing and Communication Systems (MCCS 2017); 2019; 281-293. Springer Singapore. https://doi.org/10.1007/978-981-10-8234-4_25
40. Gil JY, Kimmel R. Efficient dilation, erosion, opening, and closing algorithms. IEEE Transactions on Pattern Analysis and Machine Intelligence. 2002; 24(12):1606-17. https://doi.org/10.1109/TPAMI.2002.1114852
41. Jayaraman E, Esakkirajan S, Veerakumar. Digital Image Processing; 2010.
42. Bandeira D, Walter M. Highlights on weathering effects: Improving the appearance modelling of weathering effects on images. The Visual Computer. 2010; 26:965-74. https://doi.org/10.1007/s00371-010-0495-1
43. Mérillou S, Ghazanfarpour D. A survey of ageing and weathering phenomena in computer graphics. Computers and Graphics. 2008; 32(2):159-74. https://doi.org/10.1016/j.cag.2008.01.003
44. Kilian J. Simple image analysis by moments [Internet]. Open CV library documentation; 2001.
45. Mingqiang Y, Kidiyo K, Joseph R. A survey of shape feature extraction techniques. Pattern Recognit. 2008; 15(7):43-90. https://doi.org/10.5772/6237
46. Hu MK. Visual pattern recognition by moment invariants. IEEE Trans Inf Theory. 1962; 8(2):179-87. https://doi.org/10.1109/TIT.1962.1057692
47. Loncaric S. A survey of shape analysis techniques. Pattern Recognit. 1998; 31(8):983-1001. https://doi.org/10.1016/S0031-2023(97)00122-2
48. Fitzner B, Heinrichs K. Damage diagnosis at stone monuments-weathering forms, damage categories and damage indices. Acta Univ Carol, Geol. 2001; 1:12-3.
49. Wang P, Huang H. Comparison analysis on present image-based crack detection methods in concrete structures. In: 2010 3rd International Congress on Image and Signal Processing. 2010; 5:2530-2533. IEEE. https://doi.org/10.1109/CISP.2010.5647496
50. Zhang W, Zhang Z, Qi D, Liu Y. Automatic crack detection and classification method for subway tunnel safety monitoring. Sensors. 2014; 14(10):19307-28. https://doi.org/10.3390/s141019307
51. Abdel-Qader I, Abudayyeh O, Kelly ME. Analysis of edge-detection techniques for crack identification in bridges. J Comput Civ Eng. 2003; 17(4):255-63. https://doi.org/10.1061/(ASCE)0887-3801(2003)17:4(255)
52. Zhang YX, Zhao YQ, Liu Y, Jiang LQ, Chen ZW. Identification of wood defects based on LBP features. In: 2016 35th Chinese Control Conference (CCC). 2016; 4202-4205. IEEE. https://doi.org/10.1109/ChiCC.2016.7554010
53. Saini A, Gupta T, Kumar R, Gupta AK, Panwar M, Mittal A. Image-based Indian monument recognition using convoluted neural networks. In: 2017 International Conference on Big Data, IoT and Data Science (BID). 2017; 138-142. IEEE. https://doi.org/10.1109/BID.2017.8336587
54. Chaiyasarn K, Sharma M, Ali L, Khan W, Poovarodom N. Crack detection in historical structures based on convolutional neural network. GEOMATE Journal. 2018; 15(51):240-51. https://doi.org/10.21660/2018.51.35376
55. Islam MM, Kim JM. Vision-based autonomous crack detection of concrete structures using a fully

convolutional encoder-decoder network. Sensors. 2019; 19(19):4251. https://doi.org/10.3390/s19194251
56. Aslam Y, Santhi N, Ramasamy N, Ramar K. Localization and segmentation of metal cracks using deep learning. J Ambient Intell Humaniz Comput. 2021; 12:4205-13. https://doi.org/10.1007/s12652-020-01803-8
57. Feng C, Zhang H, Wang H, Wang S, Li Y. Automatic pixel-level crack detection on dam surface using deep convolutional network. Sensors. 2020; 20(7):2069. https://doi.org/10.3390/s20072069